Landau Levels and Quantum Hall Effect in Graphene Superlattices

Cheol-Hwan Park,[1,2] Young-Woo Son,[3] Li Yang,[1,2] Marvin L. Cohen,[1,2] and Steven G. Louie[1,2,*]

[1]*Department of Physics, University of California, Berkeley, California 94720, USA*
[2]*Materials Sciences Division, Lawrence Berkeley National Laboratory, Berkeley, California 94720, USA*
[3]*School of Computational Sciences, Korea Institute for Advanced Study, Seoul 130-722, Korea*

(Received 31 March 2009; published 24 July 2009)

We show that, when graphene is subjected to an appropriate one-dimensional external periodic potential, additional branches of massless fermions are generated with nearly the same electron-hole crossing energy as that at the original Dirac point of graphene. Because of these new zero-energy branches, the Landau levels at charge neutral filling become $4(2N + 1)$-fold degenerate (with $N = 0, 1, 2, \ldots$, tunable by the potential strength and periodicity) with the corresponding Hall conductivity σ_{xy} showing a step of size $4(2N + 1)e^2/h$. These theoretical findings are robust against variations in the details of the external potential and provide measurable signatures of the unusual electronic structure of graphene superlattices.

DOI: 10.1103/PhysRevLett.103.046808 PACS numbers: 73.43.Cd, 73.50.−h, 73.61.Wp

The physical properties of graphene [1–3] are currently among the most actively investigated topics in condensed matter physics. Graphene has the unique feature that the low-energy charge carriers are well described by the two-dimensional (2D) massless Dirac equation, used for massless neutrinos, rather than by the Schrödinger equation [2,3]. Moreover, graphene is considered to be a promising candidate for electronics and spintronics applications [4].

It has been shown that, because of their gapless energy spectrum and chiral nature, the charge carriers in graphene are not hindered by a slowly varying electrostatic potential barrier at normal incidence [5], analogous to the Klein tunneling effect predicted in high-energy physics. Direct evidences of Klein tunneling through a single barrier in graphene [5] have been observed in recent experiments [6,7].

Application of multiple barriers or periodic potentials, either electrostatic [8–12] or magnetic [13–16], to graphene has been shown to modulate its electronic structure in unique ways and lead to fascinating new phenomena and possible applications. Periodic arrays of corrugations [17–19] have also been proposed as graphene superlattices (GSs).

Experimentally, different classes of GSs have been fabricated recently. Patterns with periodicity as small as 5 nm have been imprinted on graphene through electron-beam induced deposition of adsorbates [20]. Epitaxially grown graphene on the (0001) surface of ruthenium [21–25] and that on the (111) surface of iridium [26–28] also show superlattice patterns with ~3 nm lattice period. The amplitude of the periodic potential applied to graphene in these surface systems has been estimated to be in the range of a few tenths of an electron volt [22]. Fabrication of periodically patterned gate electrodes is another possible way of making GSs with periodicity close to or larger than ~20 nm.

The quantum Hall plateaus in graphene take on the unusual values of $4(l + 1/2)e^2/h$ where l is a non-negative integer [29]. The factor 4 comes from the spin and valley degeneracies. In bilayer graphene, the quantum Hall plateaus are at $4le^2/h$ with l a positive integer [30]. These unconventional quantum Hall effects have been experimentally verified [2,3,31], providing evidences for 2D massless particles in graphene and massive particles in bilayer graphene.

In this Letter, we investigate the Landau levels (LLs) and the quantum Hall effect in GSs formed by the application of a one-dimensional (1D) electrostatic periodic potential and show that they exhibit additional unusual properties. We find that, for a range of potential shapes and parameters, new branches of massless fermions are generated with electron-hole crossing energy the same as that at the original Dirac point of pristine graphene. These additional massless fermions affect the LLs qualitatively. In particular, the LLs with energy corresponding to the Fermi energy at charge neutrality (i.e., zero carrier density) become $4(2N + 1)$-fold degenerate ($N = 0, 1, 2, \ldots$), depending on the strength and the spatial period of the potential (pristine graphene corresponds to $N = 0$). Accordingly, when sweeping the carrier density from electronlike to holelike, the quantum Hall conductivity in such a GS is predicted to show an unconventional step size of $4(2N + 1)e^2/h$ that may be tuned by adjusting the external periodic potential.

In our study, the electronic structure of the GSs is evaluated using the methods developed in Ref. [9]; we evaluate the band structure of the GS numerically by solving the 2D massless Dirac equation with the external periodic potential included using a plane wave basis. Similarly, to obtain the LLs, the eigenstates of the GSs under an external perpendicular magnetic field are expanded with plane waves. We work in a Landau gauge

with the vector potential depending on the position coordinate along the direction of the periodicity of the GS, and a zigzag form for the vector potential with a very large artificial periodicity (large compared to the GS periodicity) is employed to mimic a constant magnetic field near the origin in position space [32]. We have checked that the LLs are converged in energy to within less than 1% with respect to the size of the supercell for the vector potential and the kinetic energy cutoff for the plane waves. The size of the largest supercell and that of the smallest sampling distance in real space used are 400 and 0.05 in units of a single unit cell, respectively.

Figure 1(a) shows a GS formed by a Kronig-Penney type of electrostatic potential periodic along the x direction, with lattice parameter L and barrier width $L/2$. Remarkably, unlike that in graphene [Fig. 1(b)], the band structure in a GS [Fig. 1(c)] can have, depending on the potential barrier height U_0, more than one Dirac point with $k_x = 0$ having exactly the same electron-hole crossing energy [33]. As Fig. 1(c) shows, the number of Dirac points for this type of GSs increases by two (without considering the spin and valley degrees of freedom) whenever the potential amplitude exceeds a value of

$$U_0^N = 4\pi N\hbar v_0/L \tag{1}$$

with N a positive integer. The value of the potential barrier given in Eq. (1) corresponds to special GSs in which the group velocity along the k_y direction vanishes for charge carriers whose wave vector is near the original Dirac cone [e.g., the Dirac cone at the center in Fig. 1(c)] [34,35]. All the findings in this study apply in general to GSs made from a periodic potential which has both even and odd symmetries, like a sinusoidal type of potential. The results for GSs whose odd or even symmetry is broken are discussed in Ref. [36].

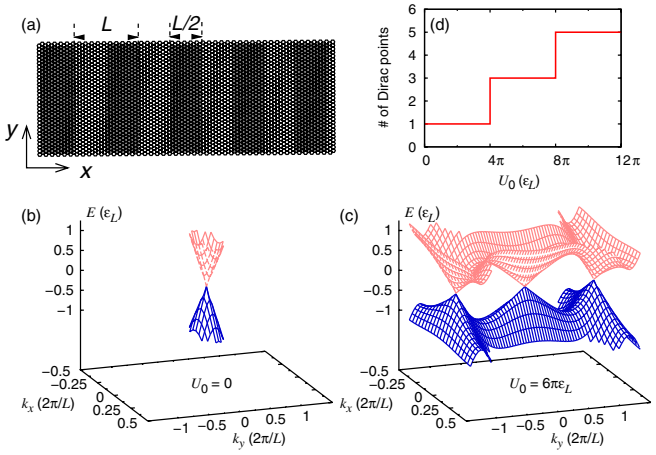

FIG. 1 (color online). (a) Schematic diagram of a Kronig-Penney type of potential applied to graphene with strength $U_0/2$ inside the gray regions and $-U_0/2$ outside with lattice period L and barrier width $L/2$. (b) Electron energy in units of ε_L ($\equiv \hbar v_0/L$; for example, if $L = 20$ nm, $\varepsilon_L = 33$ meV) versus wave vector near the Dirac point in pristine graphene. (c) The same quantity as in (b) for a GS with $U_0 = 6\pi\varepsilon_L$. (d) Number of Dirac points (not including spin and valley degeneracies) in a GS versus U_0.

Figure 2 shows the evolution of the energy of the electronic states with $k_x = 0$ for a GS depicted in Fig. 1 for several different values of U_0. As stated above, the group velocity along the k_y direction becomes zero near $k_y = 0$ when the barrier height is given by Eq. (1) [Figs. 2(c) and 2(e)]. When U_0 has a value between those specific values, the positions of the additional new Dirac points move away from the $k_y = 0$ point along the k_y direction with increasing U_0. The complex behavior of the zero-energy Dirac cones revealed by our numerical calculations cannot be derived using perturbation theory [12] because k_y is not small compared to the superlattice reciprocal lattice spacing $2\pi/L$. Moreover, the pseudospin character of these additional massless fermions [e.g., the left and the right Dirac cones (not the center one) in Fig. 1(c)] are different from that of the original massless Dirac fermions. For example, backscattering amplitude due to a slowly varying potential within one of the new cones does not vanish [36].

A natural question arising from this peculiar behavior in the electronic structure of a GS, which is topologically different from that of pristine graphene, is how the LLs are distributed. Figure 3 shows the calculated LLs of the 1D Kronig-Penney GSs depicted in Fig. 1 for various values of U_0 [37]. When the superlattice potential modulation is moderate [Fig. 3(b)], the spacings between neighboring LLs become smaller than those in pristine graphene [Fig. 3(a)], owing to a reduction in the band velocity. Once U_0 becomes larger than $4\pi\hbar v_0/L$ ($=0.4$ eV for $L =$ 20 nm), the zero-energy LLs (corresponding to zero carrier density) become three-fold degenerate [Fig. 3(d)]. An im-

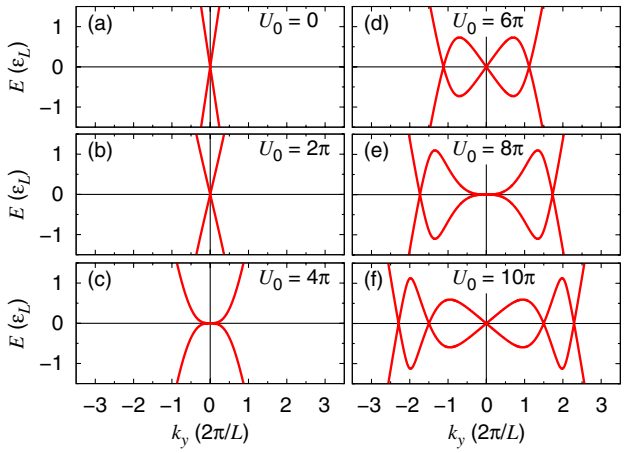

FIG. 2 (color online). Electron energy (in units of $\varepsilon_L = \hbar v_0/L$) versus k_y with $k_x = 0$ in GSs shown in Fig. 1 for several different values of barrier height U_0 (specified in each panel in units of ε_L).

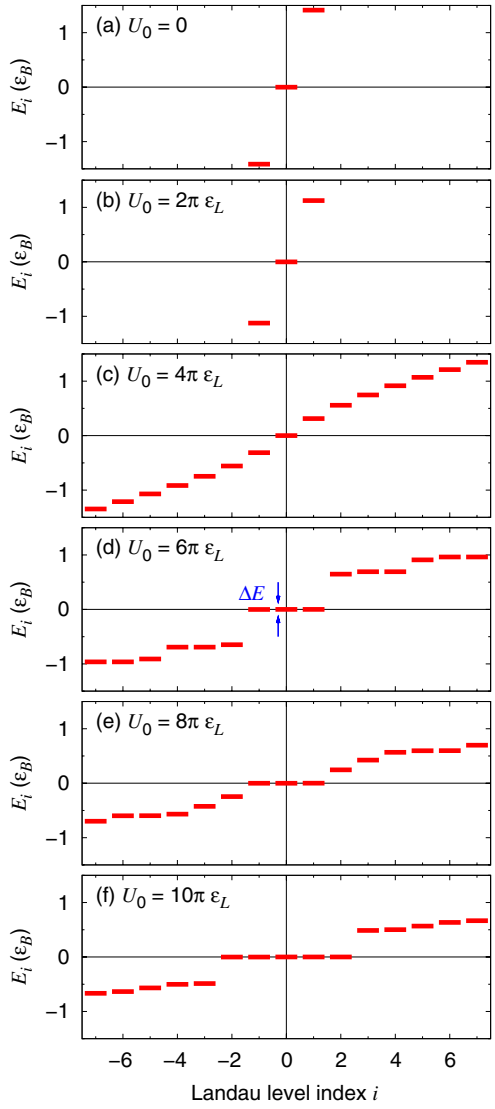

FIG. 3 (color online). Landau level energy E_i (in units of $\varepsilon_B \equiv \hbar v_0/l_B$ with $l_B = \sqrt{\hbar c/eB}$) versus the Landau level index i ($i = 0, \pm 1, \pm 2, \ldots$) in GSs formed with a 1D Kronig-Penney potential for several different values of barrier height U_0, with lattice period $L = 0.5 l_B$. The LLs now have a finite width ΔE (shown not to scale and exaggerated in the figure) arising from the k_y dependence of the energy of the electronic states in a perpendicular magnetic field [38]. Note the 3-fold and the 5-fold degeneracies around $E_i = 0$ in (d) and (f), respectively. (If the spin and valley degeneracies are considered, those become 12-fold and 20-fold, respectively.)

portant point to note is that this degeneracy is insensitive to U_0 over a range of U_0 near $6\pi\hbar v_0/L$ because the topology of the electron bands does not change with this variation [41,43]. Moreover, even though the massless particles of the different Dirac cones may have different band velocities, the degeneracy of the zero-energy LLs is not affected.

The dependence of the Hall conductivity σ_{xy} on the charge carrier density n most directly reflects the degeneracy of the LLs. Figure 4 schematically shows that, depending on the superlattice potential parameters, σ_{xy} of the GSs considered has a $4(2N+1)e^2/h$ step as the density is scanned from holelike to electronlike carriers. (We have put in the additional factor 4 coming from the spin and valley degeneracies in this discussion and in Fig. 4.) Because the degeneracy of the LLs in the 1D GSs is insensitive to a variation in U_0, this qualitative difference in σ_{xy} of the 1D GSs from that of pristine graphene (Fig. 4) is expected to be robust, and will provide a measurable signature of the unique electronic structure of the 1D GSs.

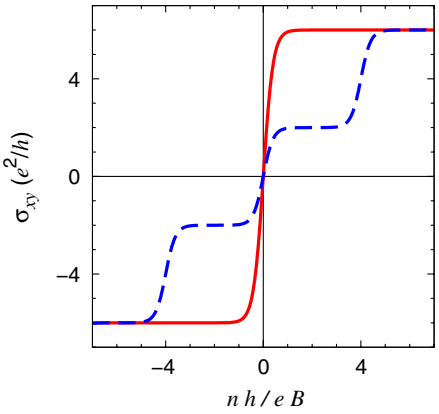

FIG. 4 (color online). Hall conductivity σ_{xy} versus carrier density (with an artificial broadening for illustration) for a 1D Kronig-Penney GS with U_0 near $6\pi\hbar v_0/L$ (solid red line) is compared to that of pristine graphene (dashed blue line).

In conclusion, we have shown that the electronic structure of 1D graphene superlattices can have additional Dirac cones at the same energy as the original cones at the K and K' points of pristine graphene. These new massless particles contribute to a $4(2N+1)$-fold degeneracy in the zero-energy Landau levels, whose signature is reflected in a $4(2N+1)e^2/h$ Hall conductivity step where $N = 0, 1, 2, \ldots$ depending on the superlattice potential parameters. This feature of the electronic structure of the 1D graphene superlattices gives rise to new properties for the quantum Hall effect. Equally important, these new phenomena may provide a direct way to characterize the peculiar electronic structure of these systems experimentally.

C.-H. P. thanks D. Novikov and J. D. Sau for fruitful discussions. This work was supported by NSF Grant No. DMR07-05941 and by the Director, Office of Science, Office of Basic Energy Sciences, Division of Materials Sciences and Engineering Division, U.S. Department of Energy under Contract No. DE- AC02-05CH11231. Y.-W. S. was supported by the KRF (KRF 2008-314-C00111) and Quantum Metamaterials Research Center (No. R11-2008-053-01002-0) through the KOSEF funded by the MEST. Computational resources have been provided by NERSC and TeraGrid.

Note added.—Recently, we became aware of theoretical work [44] confirming the newly generated massless fermions reported in this manuscript, with applications to transport properties.

*sglouie@berkeley.edu

[1] C. Berger *et al.*, Science **312**, 1191 (2006).
[2] K. S. Novoselov *et al.*, Nature (London) **438**, 197 (2005).
[3] Y. Zhang, J. W. Tan, H. L. Stormer, and P. Kim, Nature (London) **438**, 201 (2005).
[4] X. Wu *et al.*, Phys. Rev. Lett. **101**, 026801 (2008).
[5] M. I. Katsnelson, K. S. Novoselov, and A. K. Geim, Nature Phys. **2**, 620 (2006).
[6] N. Stander, B. Huard, and D. Goldhaber-Gordon, Phys. Rev. Lett. **102**, 026807 (2009).
[7] A. F. Young and P. Kim, Nature Phys. **5**, 222 (2009).
[8] C. Bai and X. Zhang, Phys. Rev. B **76**, 075430 (2007).
[9] C.-H. Park *et al.*, Nature Phys. **4**, 213 (2008).
[10] M. Barbier, F. M. Peeters, P. Vasilopoulos, and J. M. Pereira, Phys. Rev. B **77**, 115446 (2008).
[11] C.-H. Park *et al.*, Nano Lett. **8**, 2920 (2008).
[12] C.-H. Park *et al.*, Phys. Rev. Lett. **101**, 126804 (2008).
[13] M. RamezaniMasir, P. Vasilopoulos, A. Matulis, and F. M. Peeters, Phys. Rev. B **77**, 235443 (2008).
[14] M. RamezaniMasir, P. Vasilopoulos, and F. M. Peeters, Phys. Rev. B **79**, 035409 (2009).
[15] L. Dell'Anna and A. DeMartino, Phys. Rev. B **79**, 045420 (2009).
[16] S. Ghosh and M. Sharma, J. Phys. Condens. Matter **21**, 292204 (2009).
[17] F. Guinea, M. I. Katsnelson, and M. A. H. Vozmediano, Phys. Rev. B **77**, 075422 (2008).
[18] T. O. Wehling, A. V. Balatsky, M. I. Katsnelson, and A. I. Lichtenstein, Europhys. Lett. **84**, 17 003 (2008).
[19] A. Isacsson, L. M. Jonsson, J. M. Kinaret, and M. Jonson, Phys. Rev. B **77**, 035423 (2008).
[20] J. C. Meyer, C. O. Girit, M. F. Crommie, and A. Zettl, Appl. Phys. Lett. **92**, 123110 (2008).
[21] S. Marchini, S. Günther, and J. Wintterlin, Phys. Rev. B **76**, 075429 (2007).
[22] A. L. Vazquez de Parga *et al.*, Phys. Rev. Lett. **100**, 056807 (2008).
[23] Y. Pan *et al.*, arXiv:0709.2858v1.
[24] P. W. Sutter, J.-I. Flege, and E. A. Sutter, Nature Mater. **7**, 406 (2008).
[25] D. Martoccia *et al.*, Phys. Rev. Lett. **101**, 126102 (2008).
[26] J. Coraux, A. T. N'Diaye, C. Busse, and T. Michely, Nano Lett. **8**, 565 (2008).
[27] A. T. N'Diaye *et al.*, New J. Phys. **10**, 043033 (2008).
[28] I. Pletikosić *et al.*, Phys. Rev. Lett. **102**, 056808 (2009).
[29] V. P. Gusynin and S. G. Sharapov, Phys. Rev. Lett. **95**, 146801 (2005).
[30] E. McCann and V. I. Fal'ko, Phys. Rev. Lett. **96**, 086805 (2006).
[31] K. S. Novoselov *et al.*, Nature Phys. **2**, 177 (2006).
[32] The zigzag form of the vector potential we used results in the perpendicular magnetic field of a uniform strength pointing along the $+z$ direction for half the artificial periodicity and along the $-z$ direction for the other half.
[33] Note that these additional massless fermions with $k_x = 0$ are different from those generated at the supercell Brillouin zone boundaries discussed in Ref. [12].
[34] The group velocity along the k_y direction is given by $v_y = v_0 \int_{-L/2}^{L/2} e^{i\alpha(x)} dx$ where $\alpha(x)$ for a Kronig-Penney type of superlattice is given by $\alpha(x) = U_0/\hbar v_0 \cdot (|x| - L/4)$ (see Ref. [12]). When Eq. (1) is satisfied, $v_y = 0$.
[35] The use of the Dirac equation for this problem is still valid because the new Dirac points are very close to the original Dirac point ($k_x = k_y = 0$), inside the regime where the graphene band is linear. For example, in Fig. 1(c), the new massless Dirac points appear at $k_y = 1.1 \cdot 2\pi/L = 0.034$ Å if $L = 20$ nm.
[36] See EPAPS Document No. E-PRLTAO-103-023932. For more information on EPAPS, see http://www.aip.org/pubservs/epaps.html.
[37] When a vector potential $\mathbf{A}(x) = Bx\hat{\mathbf{y}}$ is used, the shift in the center of a Landau state along the x direction is proportional to k_y; hence, in a 1D superlattice periodic along x, the external periodic potential felt by a Landau state varies with k_y, resulting in a finite Landau band width ΔE (Ref. [38]). However, if the level spacing between LLs is much larger than ΔE, the signature of these LLs can be measured from experiments, as in graphene (Refs. [39,40]). In our case, we have checked that for the zero-energy LLs plotted in Fig. 3, as long as $l_B > L$, ΔE is smaller than 0.2% of ε_B. Thus, in the conditions considered here, Landau bands can be considered as discrete levels, i.e., LLs.
[38] R. W. Winkler, J. P. Kotthaus, and K. Ploog, Phys. Rev. Lett. **62**, 1177 (1989).
[39] C.-H. Park and S. G. Louie, Nano Lett. **9**, 1793 (2009).
[40] M. Gibertini *et al.*, Phys. Rev. B **79**, 241406(R) (2009).
[41] The effect of up to ~10% disorder in the on-site potential of graphene on the LL broadening is small (Ref. [42]). Since the low-energy electronic band structure of a GS can effectively be decomposed into a finite number of Dirac cones, we expect that the LLs in GSs with moderate disorder can be observed.
[42] W. Zhu *et al.*, Phys. Rev. Lett. **102**, 056803 (2009).
[43] For a Kronig-Penney superlattice with $L = 20$ nm and $l_B = 2L$ (corresponding to $B = 0.4$ T), the magnetic energy ε_B is 17 meV. In this case, temperature has to be lowered to observe the LL quantization.
[44] L. Brey and H. A. Fertig, this issue, Phys. Rev. Lett. 103, 046809 (2009).